

# Is the FIP effect present inside solar photospheric magnetic flux tubes?

V.A. Sheminova<sup>1</sup> and S.K. Solanki<sup>2,3</sup>

<sup>1</sup> Main Astronomical Observatory of Ukrainian NAS, Goloseevo, 252650 Kiev-22, Ukraine

<sup>2</sup> Institute of Astronomy, ETH-Zentrum, 8092 Zürich, Switzerland

<sup>3</sup> Max-Planck-Institute of Aeronomy, 37191 Katlenburg-Lindau, Germany

Received 7 May 1999 / Accepted 8 September 1999

**Abstract.** The first determination of the elemental composition in the photospheric layers of solar magnetic flux tubes is described. Stokes  $I$  and  $V$  profiles of 13 elements observed in solar active region plage and in the network are analysed. The abundances are obtained for elements with high (C, O) and low (Al, Ca, Cr, Na, Ni, Sc, Si, Ti, Y, Zn) first ionization potential (FIP) in order to investigate to what extent the abundance anomalies observed in the upper solar atmosphere (FIP-effect) are already present in the photospheric layers of flux tubes, which are the source of much of the gas in the upper atmosphere. Various sources of error are considered and the uncertainties introduced by them are estimated. There are hints of a weak FIP-effect in the flux tubes, corresponding to an overabundance of a factor of 1.1–1.2 of the low-FIP elements relative to high-FIP elements, as compared to the quiet photosphere. However, our data set a firm upper limit of 1.3–1.6 on this factor, which is well below the enhancement seen in many parts of the upper solar atmosphere.

**Key words:** Sun: abundances – line: formation – Sun: photosphere – Sun: magnetic fields

## 1. Introduction

It is well established that in the solar corona, in the slow solar wind and among solar energetic particles the abundances of elements with first ionization potential (FIP) below 10 eV are enhanced relative to those with higher first ionization potential when compared to the abundance ratio measured in the photosphere. This variation of relative solar abundances in different atmospheric regions is called the FIP effect (see, e.g., Meyer 1985; von Steiger & Geiss 1989; Reames et al. 1994; Feldman & Laming 1994; Sheeley 1996; Bochsler 1998; Feldman 1998; Geiss 1998, for reviews).

There is as yet no single generally accepted physical mechanism for the FIP effect. However, the idea underlying most theoretical approaches is that the segregation of high and low FIP elements takes place in the chromosphere or possibly the transition region (e.g., Henoux 1998). Nevertheless, it is worthwhile also to consider alternatives.

*Send offprint requests to:* S.K. Solanki (solanki@astro.phys.ethz.ch)

Here we investigate the possibility that the segregation has (partly or completely) already taken place in the photospheric layers of magnetic features, so called magnetic elements, thought to be composed of magnetic flux tubes (e.g., Solanki 1993). Such an effect could reproduce the observed FIP effect, since in the chromosphere the magnetic elements expand, forming a magnetic canopy (Giovanelli & Jones 1982, Solanki & Steiner 1990), and finally fill the whole upper atmosphere, so that the gas exhibiting the FIP effect is connected in the photosphere almost exclusively to the magnetic elements and to sunspots. Note that even if photospheric flux tubes exhibit a FIP effect of the same magnitude as witnessed in the upper solar atmosphere, we would still not expect it to be noticeable in standard photospheric abundance determinations, because magnetic elements cover only 1% or less of the solar surface in photospheric layers.

Even if magnetic elements were to exhibit no FIP effect, an analysis of the elemental abundances in magnetic elements still provides a firm lower boundary condition for any model of FIP segregation in the chromosphere. In fact, to our knowledge elemental abundances have never been determined in flux tubes before (with the exception of sunspots, which are not studied here).

In the present paper we determine abundances of elements inside magnetic features relative to the iron abundance there. As we shall explain in Sect. 3, it is currently not possible to obtain absolute abundances. However, this is not a serious disadvantage in the context of the FIP effect, which concerns relative abundance differences.

## 2. Observational data and selected spectral lines

The observations were made on April 29–30, 1979 with the McMath-Pierce facility and the 1m Fourier Transform Spectrometer (FTS) polarimeter of the National Solar Observatory at Kitt Peak. The data consist of Stokes  $I$  and  $V$  spectra with a spectral resolving power of  $\lambda/\Delta\lambda = 360\,000$ – $420\,000$ , a noise level of approximately  $10^{-4}$  in units of the continuum intensity,  $I_c$ , and a spatial resolution of approximately  $10''$ . A detailed description of these data is given by Stenflo et al. (1984). Here we analyse four spectrograms, 2 each observed in the network

(identified as FTS2 and FTS3) and in an active-region plage (FTS4, FTS5). Together FTS2 and FTS3, respectively FTS4 and FTS5 cover a wavelength range from 457.4 to 685.8 nm. The overlapping wavelength ranges between FTS2 and FTS3, respectively FTS4 and FTS5 were used to give the  $V$  profiles in both spectra referring to the same kind of solar region a common polarisation scale, corresponding to the same magnetic filling factor (see Solanki et al. 1986). The filling factor is the fraction of the surface area covered by magnetic field.

We have selected unblended lines of different elements within this wavelength range using the line list of Gurtovenko & Kostik (1989). After individually checking all the selected Stokes  $V$  profiles, some lines were excluded from the initial list due to the presence of small blends, or the weakness of the Stokes  $V$  signal, which make them susceptible to noise. The weak lines (with relative depth  $d < 0.1$ , where  $d = 1 - I_l/I_c$ ) are most affected by noise. They have generally been dropped, although a few weak lines of O and C have been retained because these elements have no lines with  $d > 0.1$  in the observed wavelength range. On the other hand, the strong lines ( $d > 0.75$ ,  $W > 85$  mÅ) are affected by saturation and NLTE effects, making them relatively unreliable abundance indicators. They have therefore also been dropped. Our final list consists of 93 spectral lines of 13 elements. The elements, their FIP and the number of lines analysed for each element are listed in Table 1. Unfortunately, only 2 elements, C and O, have a FIP  $> 10$  eV, since the present data set was not observed with the aim of deriving abundances. Nevertheless, it is unique in the sense that no other Stokes  $V$  spectrum combining such low noise with such a wide wavelength range has been obtained before or since.

### 3. Analysis technique, calculations and results

Our determination of the element abundances is based on the assumption of LTE and makes use of empirical models of the solar network (which we shall call NET) and plage flux tubes (PLA) constructed using Fe I, Fe II and C I lines (Solanki & Brigljević 1992), as well as the standard quiet sun atmosphere (HSRA) of Gingerich et al. (1971). The HSRA has been preferred over newer models since the flux-tube models were constructed relative to it. To ensure that quiet-sun profiles of stronger spectral lines are well reproduced the chromospheric part of the HSRA was changed so as to correspond to a steadily decreasing temperature with height (Solanki 1986). The Stokes profile calculations are carried out with a modified version of the Stokes radiative transfer code described by Sheminova (1990), which is based on a code written by Landi Degl'Innocenti (1976). The thin-tube approximation is used to describe the field strength stratification and shape of the flux tubes. The profiles are calculated along a set of 30 vertical rays piercing the cylindrical model flux tube at different radial distances from its axis using the scheme of Solanki & Roberts (1991). The line profiles formed along each of the rays are weighted according to the area on the solar disk which that ray represents and then added together to give a combined line profile which is compared with

the spatially unresolved observations (we call this procedure 1.5-D radiative transfer).

A height-independent micro- and macroturbulence of  $1 \text{ km s}^{-1}$  and  $2 \text{ km s}^{-1}$ , respectively, were introduced in the flux tubes, and of  $0.8 \text{ km s}^{-1}$  and  $1.7 \text{ km s}^{-1}$  in the quiet sun. The empirical factor to the Van der Waals damping constant, calculated using the formula given by Unsöld (1955), is chosen to be  $\delta_{\Gamma} = 2.5$ . These are the same values as those used to construct the empirical flux tube models we use for the line calculations (Solanki 1986; Solanki & Brigljević 1992). However, we have also tested the influence of varying these and other parameters (see Sect. 4). The Landé factors and splitting patterns of the selected lines of Al, C, O, Na, Si, Ca, Y, Zn have been determined assuming LS coupling. For Sc, Ti, Cr, Fe, Ni the empirical values of  $g_l$  and  $g_u$ , taken from the tables of Sugar & Corliss (1985), were employed instead. Here  $g_l$  and  $g_u$  are the Landé factors of the lower and upper state of the transition. Wherever available with sufficient accuracy, i.e. of the Fe I, Ti I, and Cr I lines, the statistically weighted oscillator strengths,  $gf$ , obtained by Blackwell's group (e.g., Blackwell et al. 1982) have been used, otherwise we employed those of Gurtovenko & Kostik (1989). We have determined the amplitudes of the blue and red wings,  $a_b$ , and  $a_r$ , of the observed Stokes  $V$  profiles and found the average amplitudes  $a_V = (a_b + a_r)/2$  for each line in the network (FTS2, FTS3) and in the plage (FTS4, FTS5). The central line depths observed in the quiet sun were taken from Gurtovenko & Kostik (1989).

In a first step we determined the element abundances for the quiet photosphere by fitting the observed central depths of all selected lines using the HSRA model. The obtained abundances,  $A_{\text{HSRA}}$ , as well as their standard deviation are listed in the 4th column of Table 1. The remaining columns list the following: The element and ion, the corresponding first ionization potential, element abundances derived using 1.5-D radiative transfer in the network and in plages with the NET and PLA models of Solanki & Brigljević (1992) and with the plage flux-tube model (PLAOLD) of Solanki (1986) (respectively labeled  $A_{\text{NET},2}$ ,  $A_{\text{PLA},2}$  and  $A_{\text{PLAOLD},2}$ ) and abundances obtained using 1-D radiative transfer with the PLA model of Solanki & Brigljević (1992) ( $A_{\text{PLA},1}$ ). Finally, abundances taken from Grevesse & Sauval (1998) are tabulated under  $A_{\text{GREV}}$ .  $N$  is the number of analysed lines of each element.

The absence of a standard deviation value for a particular element signifies that only a single spectral line could be used. A comparison with the last column of Table 1 shows that the HSRA gives consistently too low  $A$  values compared to those published by Grevesse & Sauval (1998). The differences are on average a factor of 4–5 larger than the standard deviation and are most probably a result of the difference in temperature stratification between the HSRA and the Holweger & Müller (1974) model employed by most investigators determining photospheric abundances.

When deducing the elemental abundance inside flux tubes we are faced by a further problem. In addition to their dependence on abundance and thermal stratification, the Stokes  $V$  profiles scale almost linearly with  $\alpha \cos \gamma$ , where  $\alpha$  is the mag-

netic filling factor and  $\gamma$  is the angle between the line-of-sight and the magnetic vector. They also depend on the intrinsic magnetic field strength. To counter the latter problem the intrinsic field strength in the observed regions was determined using the Fe I 5250.2 Å (Landé  $g = 3$ ) and 5247.1 Å line pair (in the spectra FTS2 and FTS4) and the Fe I 6301.5 Å and Fe I 6302.5 Å (Landé  $g = 2.5$ ) line pair (FTS3 and FTS5). Such combinations of large and small Landé factor lines provide good diagnostics of the field strength (e.g., Stenflo 1973). The dependence on the filling factor poses a more fundamental problem, however. It is not possible to simultaneously determine the filling factor and the abundances of all the elements. However, it is sufficient to assume an abundance for one of the elements and to determine the abundances of all the other elements relative to it. Since the flux tube thermal stratifications were derived mainly on the basis of Fe I and II lines assuming an iron abundance of 7.46 (corresponding roughly to the quiet sun value) we have fixed the iron abundance to this value for the current analysis as well.

We have then constructed ratios between the  $V$  amplitudes of each line of each element and of each Fe I and II line. By fixing the iron abundance to  $A_{\text{Fe}} = 7.46$  and comparing calculated with observed  $V$  ratios we then obtained estimates of the abundance of a given element separately from each single line ratio involving lines of this element in the numerator. These abundances, after averaging over all ratios involving a particular element, are presented in Table 1 (columns 5–8). Note that  $A_{\text{Element}} \equiv \log(N_{\text{Element}}/N_H + 12)$ .

The iron abundances listed in columns 5–8 of Table 1 require explanation. These values were determined separately from Fe I lines and Fe II lines in the same way as the ones of the other elements. Hence the abundance of, e.g., Fe I is determined by forming the ratio of the  $V$  profile of each Fe I line with each Fe I and II line. The abundance of the latter (i.e. the lines in the denominator) is fixed at 7.46, while that of the former is varied until the computed line ratios correspond to the observed values. In this way one obtains an abundance value from each line ratio. The abundances obtained from ratios involving Fe I in the numerator are then averaged together to give the Fe I abundance, similarly those involving Fe II. The Fe I and II abundances deduced in this manner differ from the assumed iron abundance in our flux tube models (7.46) due to differences between Fe I and II lines [note that  $A(\text{Fe I}) \leq 7.46 < A(\text{Fe II})$  for all models, except NET, for which  $A(\text{Fe I}) \approx A(\text{Fe II})$ ].

We also considered the possibility of using the areas under the  $V$  profile blue and red lobes instead of their amplitude. We decided against their use, however, since in the network the noise in the wings of the observed profiles affects approximately half of the lines from our list with sufficient severity to render them of limited use.

#### 4. Uncertainties in the analysis

The root-mean-square error estimates tabulated in Table 1 basically reflect the scatter in abundance values as derived from one spectral line to that derived from the next. Note that since each spectral line of an element gives multiple abundances, each

relative to a different line of iron, an error estimate can also be given for O I, although only a single O I line was analysed. On average, these errors are 0.03 dex in the quiet photosphere and 0.11 dex inside flux tubes. In addition to the statistical errors indicated in Table 1 the determination of abundances in magnetic elements is plagued by further uncertainties. The difference between  $A(\text{Fe I})$  and  $A(\text{Fe II})$  gives one measure of these uncertainties. This difference is found to be smaller than the tabulated error estimates.

To uncover other sources of uncertainty we carry out test calculations. We estimated the errors introduced by the uncertainties of such input parameters as the damping enhancement factor,  $\delta_{\Gamma}$ , microturbulence,  $V_{\text{mic}}$ , and macroturbulence,  $V_{\text{mac}}$ , by carrying out the abundance analysis for different values of these parameters (cf. Kostik et al. 1996). They are found to influence the abundances by no more than 0.05, 0.02 and 0.05 dex, respectively, as can be judged from Table 2. In the second column the abundance calculated in 1-D with the PLA model,  $\delta_{\Gamma} = 2.5$ ,  $V_{\text{mic}} = 1 \text{ km s}^{-1}$  and  $V_{\text{mac}} = 2 \text{ km s}^{-1}$  is tabulated for reference. In the remaining columns we list the abundances determined for the same set of parameters with the exception of the parameter listed at the head of that column.

The derived abundances also depend on the atmospheric model used, of course. This problem is particularly acute in the case of magnetic elements, due, firstly, to the large uncertainty in the thermal stratification of the empirical models used and, secondly, to the fact that this thermal structure is based on lines from only 1–2 elements and thus itself depends on the abundances assumed during its construction. To check the influence of the model atmospheres on the abundance determination, we repeated all computations, in 1.5-D, with the plage flux-tube model of Solanki (1986), which has a higher temperature in the lower photosphere than the plage atmosphere of Solanki & Brigljević (1992) used elsewhere in this paper. The results are listed in Table 1 under the column headed  $A_{\text{PLAOLD},2}$ . In general, the abundances  $A_{\text{PLA},2}$  differ from  $A_{\text{PLAOLD},2}$  by less than  $\pm 0.05$  dex. In the models of Solanki & Brigljević (1992) the elements with lines formed mainly in the deeper layers have larger abundances relative to the model of Solanki (1986), and vice versa for elements with lines formed in the higher layers. The largest effect is seen for C I (0.21 dex) and Fe II (0.06 dex), whose spectral lines are formed particularly deep (at least the ones in our list). The uncertainty in thermal stratification, we conclude, is an important source of (relative) abundance uncertainty for these elements.

In order to test the importance of multiray (1.5-D) radiative transfer we redid the analysis employing spectra calculated along a single ray in the flux tube, i.e. assuming that the flux tube model is plane parallel. The results are listed under  $A_{\text{PLA},1}$  in Table 1. This difference between 1.5-D transfer along many rays ( $A_{\text{PLA},2}$ ) and single-ray transfer ( $A_{\text{PLA},1}$ ) is expected to be important, since in the former case we take into account the expansion of the flux tube with height, so that magnetic flux is conserved with height, while in the latter case it is not (recall that the field strength decreases with height, while the fraction of the solar surface covered by field increases). Therefore, if

**Table 1.** Elemental abundances derived for the quiet solar photosphere and inside magnetic flux tubes.

Element	FIP, eV	$N$	$A_{\text{HSRA}}$	$A_{\text{NET},2}$	$A_{\text{PLA},2}$	$A_{\text{PLAOLD},2}$	$A_{\text{PLA},1}$	$A_{\text{GREV}}$
Al I	5.99	2	$6.41 \pm 0.01$	$6.52 \pm 0.08$	$6.55 \pm 0.09$	$6.53 \pm 0.08$	$6.50 \pm 0.08$	$6.47 \pm 0.07$
C I	11.26	3	$8.51 \pm 0.02$	$8.50 \pm 0.12$	$8.59 \pm 0.12$	$8.38 \pm 0.09$	$8.33 \pm 0.09$	$8.52 \pm 0.06$
Ca I	6.11	6	$6.31 \pm 0.04$	$6.37 \pm 0.09$	$6.34 \pm 0.10$	$6.33 \pm 0.09$	$6.29 \pm 0.09$	$6.36 \pm 0.02$
Cr I	6.77	7	$5.54 \pm 0.04$	$5.69 \pm 0.09$	$5.55 \pm 0.10$	$5.57 \pm 0.09$	$5.50 \pm 0.09$	$5.67 \pm 0.03$
Cr II	6.77	4	$5.48 \pm 0.01$	$5.53 \pm 0.12$	$5.57 \pm 0.13$	$5.51 \pm 0.10$	$5.48 \pm 0.09$	$5.67 \pm 0.03$
Fe I	7.87	16	$7.46 \pm 0.05$	$7.46 \pm 0.10$	$7.38 \pm 0.12$	$7.42 \pm 0.11$	$7.44 \pm 0.13$	$7.50 \pm 0.04$
Fe II	7.87	14	$7.51 \pm 0.02$	$7.44 \pm 0.11$	$7.58 \pm 0.13$	$7.52 \pm 0.11$	$7.52 \pm 0.12$	$7.50 \pm 0.04$
Na I	5.14	2	$6.23 \pm 0.02$	$6.25 \pm 0.09$	$6.34 \pm 0.11$	$6.31 \pm 0.09$	$6.29 \pm 0.10$	$6.33 \pm 0.03$
Ni I	7.63	11	$6.12 \pm 0.04$	$6.32 \pm 0.11$	$6.17 \pm 0.12$	$6.17 \pm 0.10$	$6.09 \pm 0.11$	$6.25 \pm 0.04$
O I	13.62	1	8.85	— — —	$8.85 \pm 0.08$	$8.89 \pm 0.07$	$8.87 \pm 0.07$	$8.83 \pm 0.06$
Sc II	6.56	2	$2.94 \pm 0.01$	$2.86 \pm 0.08$	$2.99 \pm 0.11$	$3.00 \pm 0.09$	$3.02 \pm 0.10$	$3.17 \pm 0.10$
Si I	8.15	13	$7.55 \pm 0.03$	$7.58 \pm 0.10$	$7.61 \pm 0.12$	$7.58 \pm 0.09$	$7.55 \pm 0.11$	$7.55 \pm 0.05$
Ti I	6.92	8	$4.88 \pm 0.03$	$5.07 \pm 0.09$	$4.90 \pm 0.09$	$4.93 \pm 0.08$	$4.87 \pm 0.09$	$5.02 \pm 0.06$
Y II	6.22	3	$2.13 \pm 0.03$	$2.34 \pm 0.12$	$2.25 \pm 0.13$	$2.25 \pm 0.11$	$2.23 \pm 0.12$	$2.24 \pm 0.03$
Zn I	9.39	1	4.44	$4.51 \pm 0.09$	$4.65 \pm 0.11$	$4.60 \pm 0.09$	$4.57 \pm 0.10$	$4.60 \pm 0.08$

**Table 2.** Influence of the parameters  $\delta_{\Gamma}$ ,  $V_{\text{mic}}$  and  $V_{\text{mac}}$  on the determined abundance inside flux tubes.

Element	Reference	$\delta_{\Gamma} = 1$	$V_{\text{mic}} = 0.5$	$V_{\text{mic}} = 1.5$	$V_{\text{mac}} = 1.5$	$V_{\text{mac}} = 2.5$
Al I	$6.50 \pm 0.08$	$6.45 \pm 0.09$	$6.50 \pm 0.08$	$6.50 \pm 0.09$	$6.53 \pm 0.09$	$6.48 \pm 0.09$
C I	$8.33 \pm 0.09$	$8.28 \pm 0.08$	$8.33 \pm 0.08$	$8.32 \pm 0.09$	$8.38 \pm 0.10$	$8.29 \pm 0.08$
Ca I	$6.29 \pm 0.09$	$6.25 \pm 0.09$	$6.28 \pm 0.09$	$6.29 \pm 0.10$	$6.30 \pm 0.10$	$6.28 \pm 0.09$
Fe I	$7.44 \pm 0.13$	$7.45 \pm 0.13$	$7.45 \pm 0.13$	$7.44 \pm 0.13$	$7.45 \pm 0.13$	$7.44 \pm 0.13$
Ti I	$4.87 \pm 0.09$	$4.87 \pm 0.09$	$4.86 \pm 0.08$	$4.89 \pm 0.09$	$4.86 \pm 0.08$	$4.89 \pm 0.09$

only a single ray is used the ratio of  $V$  profiles of lines formed at greater height relative to those of lines formed deeper (e.g. Fe I vs. C I) is smaller compared to the ratio resulting from multi-ray calculations. The obtained abundance difference between these two cases ranges from 0.10 dex (lines formed in the deeper layers) to  $-0.06$  dex (the higher layers). These tests confirm the need for 1.5-D calculations.

An additional potentially important cause of errors in our analysis are enhanced NLTE-effects in magnetic flux tubes. Solanki & Steenbock (1988) have estimated the effects of departures from LTE on Fe I and II line profiles formed in the quiet sun and in flux tubes based on an extensive multilevel atom, but neglecting the geometry of flux tubes. Whereas Fe II lines show almost no difference between LTE and NLTE in all models, Fe I lines are considerably affected by the overionization of iron, their abundances being changed by up to 0.2 dex. The same is probably true for lines of other low excitation-potential elements.

We can very roughly estimate the magnitude of the NLTE effects by comparing the Fe I and the Fe II abundances derived for a given atmosphere and assuming  $\Delta A = A_{\text{NLTE}} - A_{\text{LTE}} = A_{\text{Fe II}} - A_{\text{Fe I}}$ . Since we do not expect the Fe II lines to be influenced by NLTE effects, the abundance derived using these lines should be close to those obtained after taking NLTE effects into account. It follows from Table 1 that  $\Delta A$  (HSRA) = 0.05,  $\Delta A$  (NET) =  $-0.02$ ,  $\Delta A$  (PLA) = 0.20,  $\Delta A$  (PLAOLD) = 0.10. Hence the plage flux tubes exhibit the largest NLTE effect. The smallest discrepancy is shown by the network, which may be

due to the stronger temperature induced weakening of the Stokes profiles in the network, so that they are formed lower, close to the levels at which the UV continuum arises, making them less susceptible to overionization. On the other hand, it cannot be ruled out that the values of  $\Delta A$  are not significant.

In conclusion, there appear to be four main causes for the uncertainty in our abundance determinations. These are (1) the neglect of NLTE effects, (2) the problem that only abundances relative to the Fe I abundance can be determined due to the scaling of the  $V$  profiles with the magnetic filling factor, (3) the uncertainty in the temperature stratification and geometry of flux tubes and (4) uncertainties in the damping enhancement factor and the turbulence velocity.

## 5. Discussion and conclusion

In the present investigation we have derived the abundances of 12 active-region elements relative to the iron abundance inside magnetic flux tubes in plage and in the network. In Figs. 1 and 2 we plot the ratios between the abundances in active and quiet regions, i.e.  $N_{\text{NET}}/N_{\text{HSRA}}$  and  $N_{\text{PLA}}/N_{\text{HSRA}}$  as a function of FIP and of atomic mass  $M$ , respectively.

Fig. 2 shows that there is no significant dependence of the derived abundances on atomic mass. According to Fig. 1 the low FIP element abundances inside the flux tubes relative to the quiet region are slightly enhanced, as compared with the abundances of the high FIP elements. These enhancements are approximately 0.08 dex in the network and 0.04 dex in plage

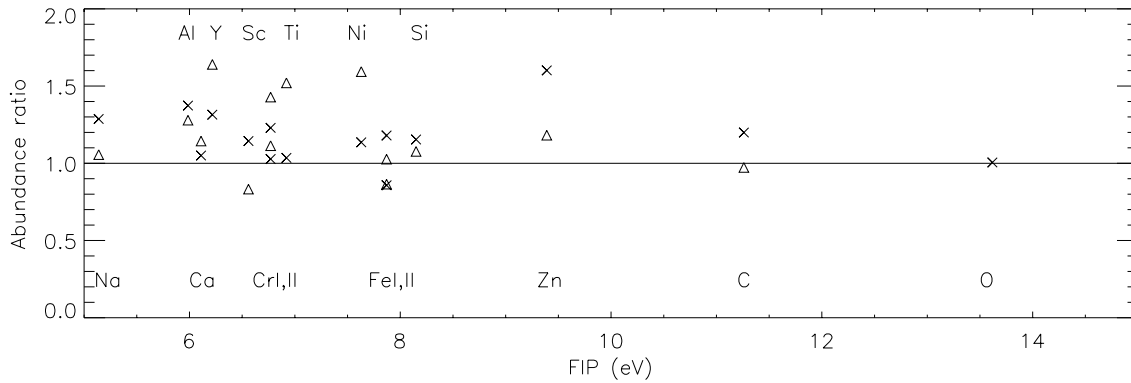


**Fig. 1.** Ratio of element abundances inside network (crosses) and plage flux tubes (triangles) relative to the quiet photosphere vs. the First Ionization Potential (FIP)

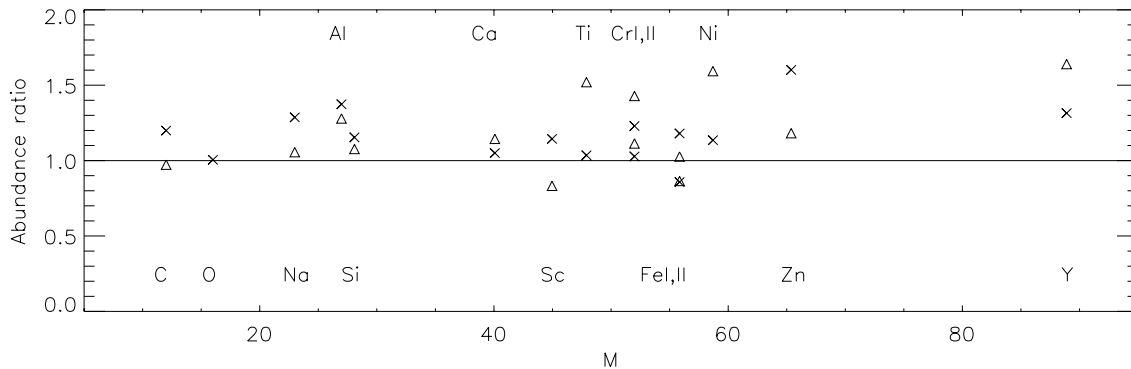


**Fig. 2.** Ratio between element abundance inside flux tubes and in the quiet photosphere as a function of atomic mass. Crosses refer to network flux tubes, the triangles to plage flux tubes

flux tubes. In view of the uncertainties inherent in the analysis these enhancements can be considered to be marginally significant only. More importantly, a  $3\sigma$  upper limit can be set on the enhancement of the abundance of low FIP elements over high FIP elements of about a factor of 1.6 in the network (corresponding to 0.2 dex) and 1.3 in the plage (corresponding to 0.11 dex). These upper limits are far lower than the factor of 4 enhancement of the abundances of low-FIP elements seen in the corona and the slow solar wind (Feldman 1998, Geiss 1998). Hence, only a very minor part of the element segregation observed in the outer solar atmosphere seems to take place in photospheric and subphotospheric layers.

An interesting investigation awaiting future effort would be to determine the height at which FIP segregation does begin to assert itself.

*Acknowledgements.* This work has been funded by the Swiss National Science Foundation under grant 7UKPJ048440. We thank A.S. Gadun for helpful discussions and R.J. Rutten for valuable comments on the manuscript.

## References

- Blackwell D.E., Petford A.D., Simmons G.J., 1982, MNRAS 201, 595  
 Bochsler P., 1998, in *Solar Composition and its Evolution – from Core to Corona*, C. Fröhlich, M.C.E. Huber, S.K. Solanki, R. von Steiger (Eds.), Kluwer, Dordrecht, p. 291  
 Feldman U., 1998, in *Solar Composition and its Evolution – from Core to Corona*, C. Fröhlich, M.C.E. Huber, S.K. Solanki, R. von Steiger (Eds.), Kluwer, Dordrecht, p. 227  
 Feldman U., Laming J.M., 1994, ApJ 434, 370  
 Geiss J., 1998, in *Solar Composition and its Evolution – from Core to Corona*, C. Fröhlich, M.C.E. Huber, S.K. Solanki, R. von Steiger (Eds.), Kluwer, Dordrecht, p. 241  
 Gingerich O., Noyes R.W., Kalkofen W., Cuny Y., 1971, Solar Phys. 18, 347  
 Giovanelli R.G., Jones H.P., 1982, Solar Phys. 79, 267  
 Grevesse N., Sauval A.J., 1998, in *Solar Composition and its Evolution – from Core to Corona*, C. Fröhlich, M.C.E. Huber, S.K. Solanki, R. von Steiger (Eds.), Kluwer, Dordrecht, p. 161  
 Gurtovenko E.A., Kostik R.I., 1989, *The Fraunhofer Spectrum and the System of Solar Oscillator Strengths*, Naukova Dumka, Kiev  
 Henoux J.-C., 1998, in *Solar Composition and its Evolution – from Core to Corona*, C. Fröhlich, M.C.E. Huber, S.K. Solanki, R. von Steiger (Eds.), Kluwer, Dordrecht, p. 215  
 Holweger H., Müller E.A., 1974, Solar Phys. 39, 19  
 Kostik R.I., Shchukina N.G., Rutten R.J., 1996, A&A 305, 325  
 Landi Degl’Innocenti E., 1976, A&AS 25, 379  
 Meyer J.P., 1985, ApJS 57, 151  
 Reames D.V., Meyer J.P., von Roseninge T.T., 1994, ApJS 90, 649  
 Sheeley N.R., 1996, ApJ 469, 423  
 Sheminova V.A., 1990, *Calculating the profiles of the Stokes Parameters of magnetoactive absorption lines in stellar atmospheres* (in Russian), Kiev (VINITI File No. 2940-V90,30 May 1990)

- Solanki S.K., 1986, A&A 168, 311  
Solanki S.K., 1993, Space Sci. Rev. 61, 1  
Solanki S.K., Brigljević V., 1992, A&A 262, L29  
Solanki S.K., Roberts B., 1991, MNRAS 256, 13  
Solanki S.K., Steenbock W., 1988, A&A 189, 243  
Solanki S.K., Steiner O., 1990, A&A 234, 519  
Solanki S.K., Pantellini F.G.E., Stenflo J.O., 1986, Solar Phys. 107, 57
- Stenflo J.O., 1973, Solar Phys. 32, 41  
Stenflo J.O., Harvey J.W, Brault J.W., Solanki S.K., 1984, A&A 73, 314  
Sugar J., Corliss C., 1985, J. Phys. Chem. Ref. Data 14, Suppl. No.2  
Unsöld A., 1955, Physik der Sternatmosphären, Springer Verlag, Berlin  
von Steiger R., Geiss J., 1989, A&A 225, 222